

MINERALOGICAL MAGAZINE

VOLUME 58 NUMBER 393 DECEMBER 1994

Use of element–mineral correlations to investigate fractionation of rare earth elements in fine-grained sediments

J. T. TEMPLE

Department of Geology, Birkbeck College, Malet Street, London WC1E 7HX, UK

AND

J. N. WALSH

Department of Geology, RHB New College, Egham Hill, Egham, Surrey TW20 0EX, UK

Abstract

Relative concentrations of elements in the minerals of fine-grained sediments can be inferred from element-mineral correlation coefficients. The technique is applied to the distribution of *REE* in Middle Ordovician shales from South Wales analysed by ICPAES, Leco C/S125 and XRD. Phosphate and chlorite show mid-*REE* enrichment; muscovite + biotite shows mid-*REE* depletion. The complementarity of the chlorite and muscovite + biotite patterns may be due to fractionation during diagenetic recrystallisation. Partial correlation analysis is used to infer the presence of zircon.

KEYWORDS: *REE*, fractionation, fine-grained sediments, element-mineral correlations.

Introduction

INVESTIGATION of the mineralogical distribution of elements in fine-grained sediments presents considerable problems because direct chemical analysis of individual minerals is usually impracticable. In the present study we describe a statistical technique for inferring element concentrations in minerals, and investigate thereby the mineralogical distribution of *REE* in some Middle Ordovician shales from South Wales.

Methodology

Theory

Let: p_i = concentration of element *A* in mineral *C* in rock specimen *i*,
 q_i = concentration of element *A* in non-*C* (the rest of specimen *i*),
 k_i = mass of mineral *C* in specimen *i*,
 $1-k_i$ = mass of non-*C* in specimen *i*,
where p_i , q_i and k_i are independent random

variables ($0 \leq p_i \leq 1$; $0 \leq q_i \leq 1$; $0 \leq k_i \leq 1$).

Then: $p_i k_i$ = mass of element A in C in specimen i ,

$q_i(1 - k_i)$ = mass of element A in non- C in specimen i ,

$p_i k_i + q_i(1 - k_i) = (p_i - q_i) k_i + q_i = m_i$
= total mass of element A in specimen i .

We can measure m_i and θk_i , where θ is a constant, and therefore from a sample of n specimens we can calculate the correlation coefficient (r) between them, i.e. between $\{(p_i - q_i) k_i + q_i\}$ and θk_i . We wish to find the relation between r and the mean values of p_i or $(p_i - q_i)$.

Writing E for the mathematical expectation or mean of a function, and ignoring the constant θ which cancels out in the calculations, we find that the covariance of $[(p - q)k + q]$ and k is:

$$\begin{aligned} & E[(p - q)k^2 + qk] - E[(p - q)k + q] E(k) \\ &= E[(p - q)k^2] + E(qk) - E[(p - q)k] E(k) - E(q) E(k) \\ &= E[(p - q)k^2] - E[(p - q)k] E(k), \text{ since } q \text{ and } k \text{ are independent,} \\ &= E(p - q) E(k^2) - E(p - q) E^2(k), \text{ since } (p - q) \text{ and } k \text{ are independent,} \\ &= E(p - q) [E(k^2) - E^2(k)]. \end{aligned}$$

If we now write $(\bar{p} - \bar{q})$ for $E(p - q)$ and σ for standard deviations, the correlation coefficient r between m and k becomes:

$$r = (\bar{p} - \bar{q}) \sigma_k / \sigma_m. \quad (1)$$

Since both σ_k and σ_m are ≥ 0 , the sign of r is determined by the sign of $(\bar{p} - \bar{q})$. Thus if:

$$(\bar{p} - \bar{q}) > 0, r > 0,$$

$$(\bar{p} - \bar{q}) < 0, r < 0.$$

Furthermore, the magnitude of r is directly proportional to the value of $(\bar{p} - \bar{q})$ normalised by σ_m .

We note three special cases:

(1) if $(\bar{p} - \bar{q}) = 0$, $r = 0$: if the concentration of the element is the same in the mineral as elsewhere (i.e. equal to the overall mean concentration), the correlation coefficient is zero;

(2) if $p_1 = p_2 = p_3 = \dots \neq 0$, and $q_1 = q_2 = q_3 = \dots = 0$, $r = +1$: if the element has constant concentration in the mineral and zero concentration elsewhere the correlation coefficient takes a limiting value of $+1$;

(3) conversely, if $p_1 = p_2 = p_3 = \dots = 0$, and $q_1 = q_2 = q_3 = \dots \neq 0$, $r = -1$: if the element has zero concentration in the mineral and constant concentration elsewhere the correlation coefficient takes a limiting value of -1 .

We now widen the model to encompass two elements (or e.g. oxides) A and B , and a mineral C . There are now 5 variables p_A , q_A , p_B , q_B and k_C , which are assumed to be independent except that p_A may be correlated with p_B , and q_A with q_B . The measured quantities are now m_A , m_B and θk_C . If

we denote the *total correlation coefficients* between these measurements by r_{AB} , r_{AC} and r_{BC} , and the *partial correlation coefficient* between m_A and m_B by $r_{AB.C}$, then

$$r_{AB} = r_{AC} \cdot r_{BC} + r_{AB.C} \cdot \sqrt{(1 - r_{AC}^2)(1 - r_{BC}^2)}. \quad (2)$$

Application

By reason of equation (1) we can use r for comparing the relative concentrations of different elements in a mineral: the mineral/element correlation coefficient is in fact analogous to the logarithm of the distribution coefficient of an element between mineral and matrix, or to *REE* concentrations 'normalised' to a standard set of concentrations, the most appropriate in the present instance being the North American Shale Composite (NASC) of 40 shales (Gromet *et al.*, 1984; McLennan, 1989, table 2). There is, however, an important conceptual difference between 'normalised' concentrations and correlation coefficients: the former are relative to a particular set of external standards, while the latter are relative to the mean concentrations in the sample of n specimens — albeit in the present case the mean concentrations are closely similar to the shale standard (Table 1). There is therefore a constraint on the correlations (as there is also on mineral/matrix distribution coefficients) that is not present in straightforward measurements of *REE* concentrations in minerals. The closeness of the reciprocal relationship between muscovite + biotite and chlorite (see below) may be accentuated by this constraint.

TABLE 1. Mean concentrations (ppm) of rare earth elements in (a) NASC shale composite (from McLennan, 1989, table 2), and (b) 31 shales from Whitland

	(a)	(b)
La	32	34.84
Ce	73	74.43
Pr	7.9	8.90
Nd	33	34.11
Sm	5.7	6.22
Eu	1.24	1.28
Gd	5.2	5.77
Dy	5.8	5.68
Ho	1.04	1.05
Er	3.4	2.76
Yb	3.1	2.67
Lu	0.48	0.45

In the extended model, if we interpret *A* as a REE and *B* as another constituent of a mineral (e.g. an oxide), then we see from equation (2) that r_{AB} (REE/oxide) and r_{AC} (REE/mineral) will be likely to have the same sign if r_{BC} (oxide/mineral) is positive. For an oxide (or other element) with a higher concentration in a mineral than in the rest of the rock (i.e. r_{BC} positive) the plot of REE/oxide correlations is therefore likely to be similar to that of REE/mineral correlations relative to the $r = 0$ line. Indeed, in the limiting case of an oxide (or element) *B* which is restricted to a mineral *C* and occurs therein in constant proportions, $r_{BC} = +1.0$ and $r_{AB.C} = 0$, so that $r_{AB} = r_{AC}$, i.e. the two plots coincide, as is approximately true for K_2O and Cr with respect to muscovite + biotite in Fig. 2a. In other cases described below the coincidence of the plots is not so exact, but the similarity is nevertheless close enough for REE/oxide or element correlations to be used in practice as proxy for REE/mineral correlations. Furthermore, by inverting equation (2) we can calculate $r_{AB.C}$, the partial correlation between *A* and *B* when the effect of mineral *C* is removed, and by extension of the process we can calculate $r_{AB.CD}$, $r_{AB.CDE}$, etc., and thereby find the partial correlation between *A* and *B* when the effects of other minerals *D*, *E*, etc., have also been removed. From the REE/element correlation patterns that remain after thus partialling out the effects of all the measured minerals, we can then infer the presence of minerals not measured by XRD.

Two practical aspects of the application of the methodology should be mentioned. Firstly, the method is based on a sample of rock specimens, not on a single specimen, and the concentrations so obtained relate to the mean relative concentrations of the elements in the mineral phases averaged over the whole sample. Although, therefore, the sample must be large enough to provide reliable estimates of correlation coefficients, it should not be so large or heterogeneous as to encompass wide divergences in the chemical composition of the minerals concerned. As with all correlation-based techniques, there is a sensitivity to outliers. Sub-sampling from the data set described below (31 specimens of black shale) suggests that reliable results can be obtained on samples of size $n = 10$.

Secondly, the method requires accurate estimates not only of chemical composition (as in single crystal studies) but also of mineralogical composition. Mineralogical composition is most conveniently assessed by X-ray diffraction (XRD) techniques as the intensities of reflections at suitable *d*-spacings. The problem is to find *d*-spacings that are unique to particular minerals and

free from interference from other minerals. The present technique, however, itself provides a check on interference, because the mineral-element correlations should accord with the mineral composition: intensities measured on a *d*-spacing supposedly representing pure quartz, for instance, should not show significant positive correlations with any of the major oxides. For this reason quartz has not been used in the analysis that follows because of interference on the two most suitable peaks, 2.28Å (calcite) and 4.26Å (feldspars). In contrast, albite (4.03 or 6.39Å) appears to give consistent results. For micas, the 4.97–5.04Å peak is interpreted as primarily an index of muscovite + biotite, although it may include contributions from paragonite and rectorite. Similarly the 14.4Å peak is interpreted as an index of chlorite, although it probably includes contributions from chlorite/smectite and chlorite/vermiculite interlayerings. In future it will probably be possible to overcome these problems by using algorithms for the automatic measurement of mineral intensities from XRD traces (e.g. Bish and Chipera, 1988; Taylor and Rui, 1992).

Application to REE distribution in black shales

The observed concentrations and mineralogical distribution of elements in black shales are the resultants of three separate signals — detrital, authigenic, and diagenetic. The low concentrations of REE in sea water suggest that the elements are relatively immobile during weathering and transport, being carried partly in heavy detrital minerals, especially zircon and titanite, and partly adsorbed on to clay particles (McLennan, 1989, pp. 175,179). REE are, however, enriched in authigenic material, e.g. ferromanganese nodules and phosphates (Fleet, 1984, pp. 360, 363). The enhancement of REE concentrations in the pore waters of reducing nearshore sediments led Elderfield and Sholkovitz (1987) to infer that REE may be mobilised during diagenesis, and the progressive down-hole depletion of REE in Japan Sea sediments (Murray *et al.*, 1991) has been attributed to this cause, as has the development of a positive Eu anomaly in Amazon deep-sea fan muds (MacRae *et al.*, 1992). It has also been suggested (Milodowski and Zalasiewicz, 1991) that there may be REE mobilisation between different sedimentary phases during diagenesis.

The present study investigates fractionation of REE between different mineral phases in some Middle Ordovician shales of which the broad outlines of the geochemistry (excluding REE) and mineralogy have already been published (Temple and Cave, 1992).

Sampling and analytical techniques

31 specimens of shale were collected at 2m stratigraphical intervals from strata belonging to the *clingani* and *linearis* graptolite zones (Middle Ordovician) in the A40(T) road cutting near Whitland [SN 1723 1691], South Wales.

ICPAES analysis was carried out on a Philips ICP polychromator (Thompson and Walsh, 1988). Sample means for the analysed oxides and elements are given in Temple and Cave, 1992, table 1 (all Fe was determined as Fe_2O_3). *REE* were analysed separately by ICPAES following cation separation (Walsh *et al.*, 1981) to obtain data on La, Ce, Pr, Nd, Sm, Eu, Gd, Dy, Ho, Er*, Yb and Lu: sample means are given in Table 1. Organic (non-carbonate) C and S were measured on a Leco C/S125 analyser. XRD analysis was carried out on a Philips PW1710 diffractometer (Roberts *et al.*, 1990, p. 272). Mineral abundances were measured as the heights above adjacent background of peaks at 4.97–5.04Å (muscovite + biotite), 6.39Å (albite) and 14.4Å (chlorite).

Results

Fig. 1 is a variate plot on the first 3 eigenvectors of the 39-variate correlation matrix based on 21 oxides and elements, 12 *REE*, organic C and S, LOI, and 3 XRD *d*-spacings. For clarity of presentation the y_2 (27.3% of trace) and y_3 (14.8%) axes are placed horizontally, and the y_1 axis (30.1% of trace) is vertical, while oxides are listed as elements. With the exceptions noted, positive inter-variate correlation coefficients greater than 0.5 (all significant at <1% two-sided level) are indicated. The plot shows the same mineralogical groupings as those of the previously published eigenvector plot without *REE* (Temple and Cave, 1992, p. 593, fig. 2). The cluster of open symbols (negative y_1 scores) at the top of the ordination represents muscovite + biotite (4.97–5.04Å) and the associated elements and oxides, i.e. K_2O , Al_2O_3 , TiO_2 , Cr, Zr, *LREE* and *HREE*. At the bottom on the left and mainly with positive y_1 scores (solid symbols) is the chlorite (14.4Å) cluster of Fe_2O_3 , MgO, Li, MnO, Cu, Co, Zn and Ni. At the bottom on the right with negative y_1 scores is the phosphate-carbonate cluster of CaO, Sr, P_2O_5 and Y, with LOI associated. Albite (6.39Å) plots near the top of the ordination, with positive y_1 scores and close to Na_2O , C and V. Ba, Sc and S are rather isolated, although Sc is linked with *LREE*, and S with Co. The *REE* form a string from *LREE* near muscovite + biotite to *MREE* between the phos-

phate and chlorite clusters (but more closely linked to the former), and then doubled back so that *HREE* again approach muscovite + biotite.

The relations of the *REE* are shown in more detail in Fig. 2a–e as curves of the correlation coefficients between the *REE* and the different minerals (and their constituent elements), the correlation coefficients being proportional to the concentrations of the *REE* relative to the sample mean concentrations (Table 1) represented by the $r=0$ line.

Elements and minerals with similar *REE* response patterns have been grouped together in Fig. 2a–e, and it will be seen that most of the elements fall into either the muscovite + biotite group (4.97–5.04Å — Fig. 2a), or the chlorite group (14.4Å — Fig. 2b), and that the patterns of the two figures are complementary: chlorite is enriched in *MREE* (Sm to Ho), while muscovite + biotite is depleted in *MREE*s and enriched in *LREE* and *HREE*. In Fig. 2a the curves for Al_2O_3 , K_2O , TiO_2 and Cr are remarkably parallel to the muscovite + biotite curve, while Zr diverges only slightly by being lower for *LREE* and higher for *HREE*. A feature of Fig. 2b is the positive Ce anomaly in members of the chlorite group. MgO is the only exception, and in this respect, as also in the high values of its *REE* correlations, it approaches the condition of the phosphate-carbonate group of elements in Fig. 2c. Members of this group (P_2O_5 , CaO, Sr and Y) resemble the chlorite group in showing *MREE* enrichment, but differ in having a negative Ce anomaly. Fig. 2d shows the correlations of albite (6.39Å), Na_2O , organic C and V, all of which are slightly concave upwards and least depleted in *HREE*. Fig. 2e shows the three remaining elements. Sc and Ba show similar upwardly biconvex curves resembling muscovite + biotite in relative depletion of middle *REE*, scandium being distinguished by showing positive correlations with all of the *REE*, presumably because of its chemical affinities to the lanthanides. Sulphur remains everywhere close to the mean line, from which it appears, however, to show consistent and non-random deviations (e.g. depletion in *LREE*).

Discussion

The most striking aspect of the *REE* concentration patterns in Fig. 2a (muscovite + biotite) and Fig. 2b (chlorite) is their complementarity. Since, however, these three minerals probably constitute between them the greater part of the Whitland samples (and probably contribute an even greater proportion of the *REE* content), and since the patterns are relative to the mean concentrations in the samples, the closeness of the complementarity

*ICPAES data for Er are probably less reliable than for other *REE* (Walsh *et al.*, 1981, p.147): they have been retained in the calculations despite producing slightly anomalous results (Fig. 2).

is probably artefactual. There are several reasons why we should beware of seeking a purely mineralogical explanation of the individual muscovite + biotite and chlorite REE patterns at Whitland. Firstly, published data on REE distributions in chlorite, muscovite and biotite (Cullers *et al.*, 1975, table 2; Roaldset, 1975, table 2; Taylor and McLennan, 1985, table 2.12; Ward *et al.*, 1992, table 2) do not show consistent enough patterns within, nor consistent enough

differences between, the three minerals, for comparisons to be made with the Whitland patterns, except for the observation that the strong LREE enrichment in muscovite + biotite at Whitland is unusual. Secondly, a large proportion of the REE content is probably adsorbed on to the surfaces and in the interspaces of the minerals, so that we do not need to consider in detail the lattice structures of the minerals. Roaldset has shown that, for micas and chlorite

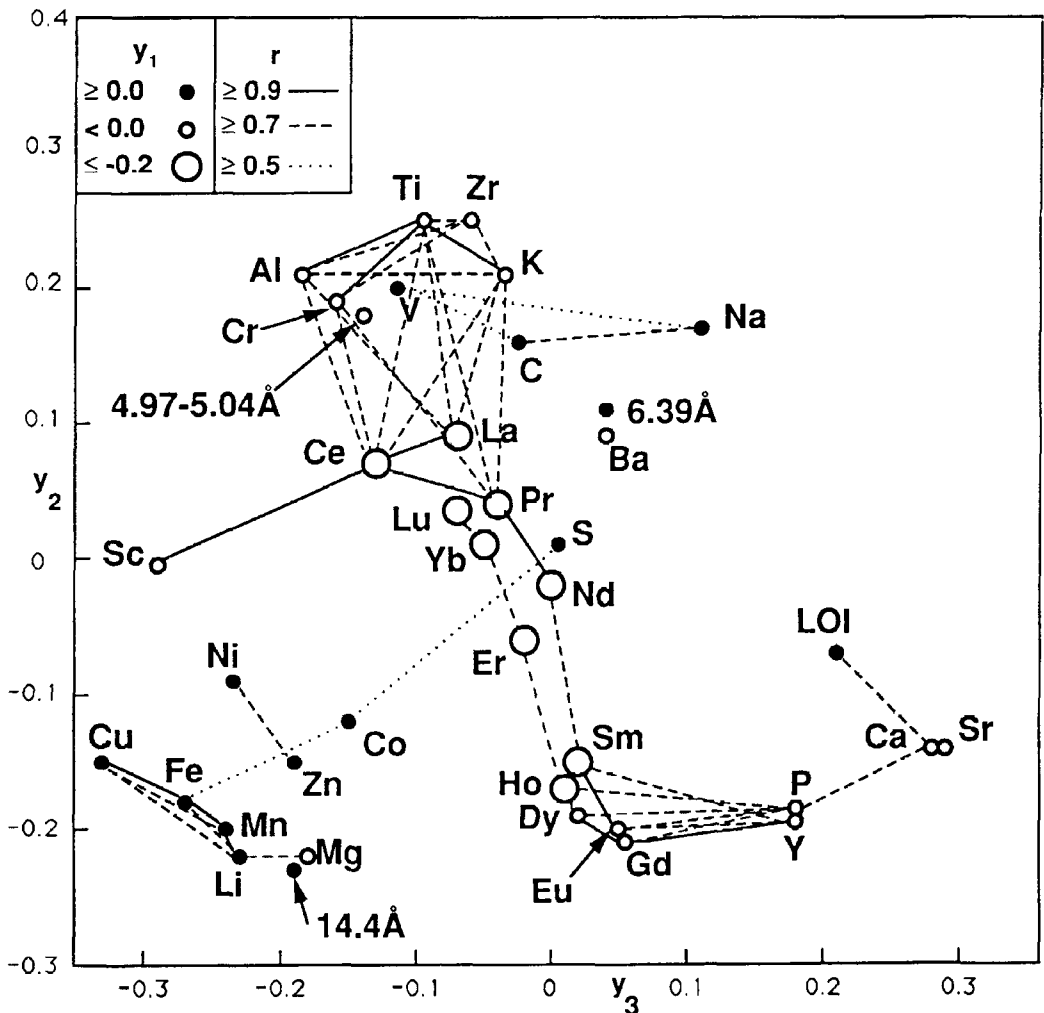
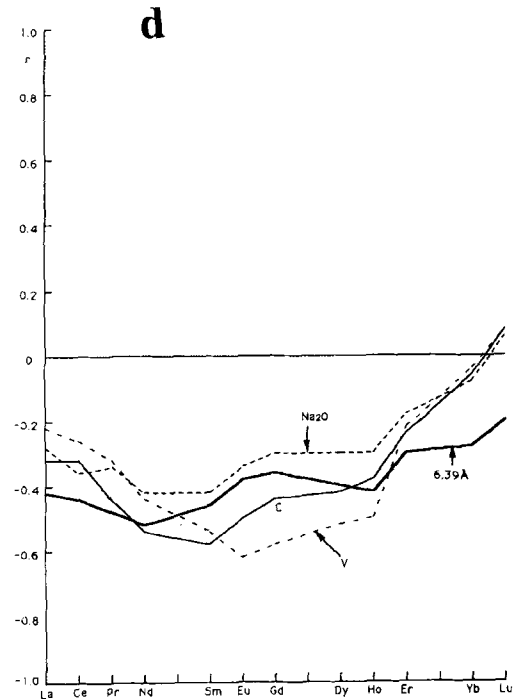
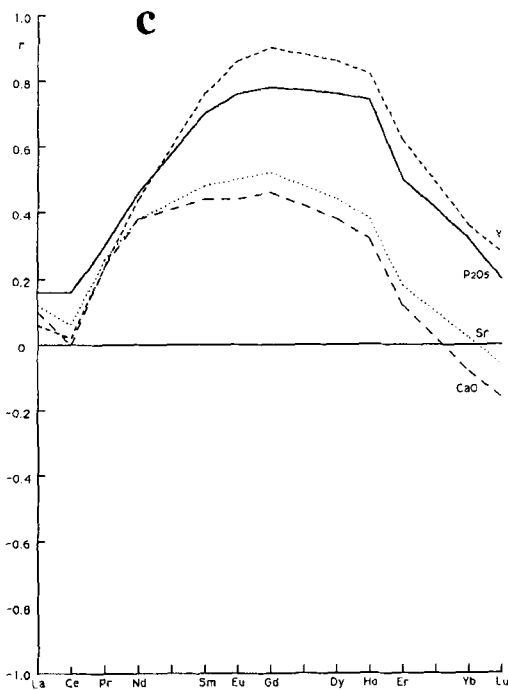
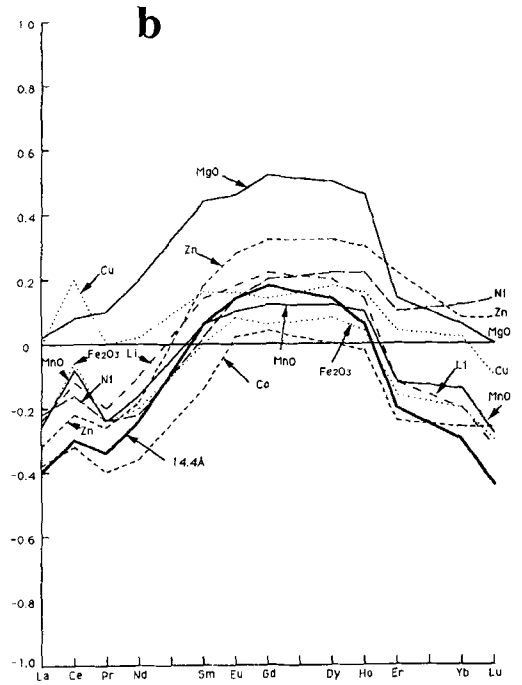
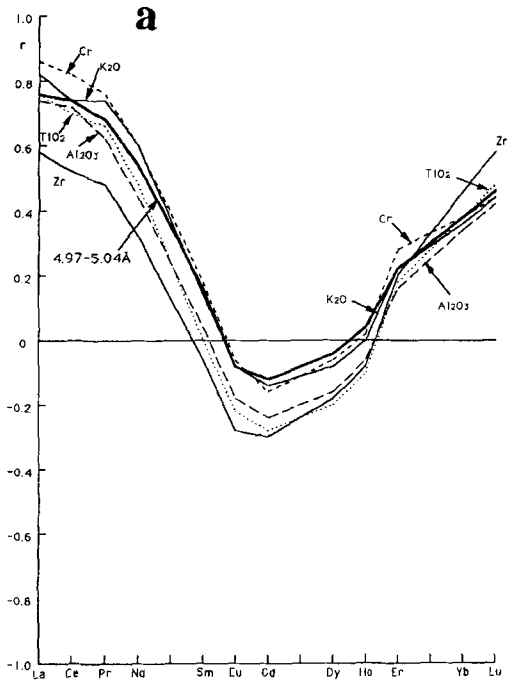


FIG. 1. Element/oxide concentrations and *d*-spacing intensities plotted on the first three eigenvectors (y_1 to y_3 – note that y_1 is perpendicular to the paper) of the 39-variate correlation matrix, based on 31 shales from Whitland. All correlations with coefficients ≥ 0.7 are shown; correlations with coefficients ≥ 0.5 are shown only for variates with no coefficients ≥ 0.7 . Some of the plotted points have been shifted slightly in the y_2/y_3 plane so as to clarify the relationships. 4.97–5.04 Å *d*-spacing represents muscovite + biotite, 6.39 Å albite, and 14.4 Å chlorite (see text).



from the Norwegian Precambrian, up to 70% of the REE content was leachable by EDTA (1975, tables 2, 3), and her figures confirm the suggestion (Erel and Stolper, 1993) that LREE are preferentially adsorbed on to surfaces. Finally, preliminary studies of three other sections of Welsh Ordovician black shales also show complementary REE patterns in muscovite+biotite and chlorite, even though the detailed patterns are not the same as at Whitland. We conclude that it is the complementarity of the Whitland muscovite+biotite and chlorite REE patterns that needs explanation, rather than the patterns themselves. This complementarity is best explained by scavenging of REE during diagenetic recrystallisation of the unfractionated precursors of the minerals: the detailed resulting patterns for muscovite+biotite and chlorite presumably depend on local compositional and diagenetic conditions.

Two aspects of the muscovite+biotite and chlorite patterns at Whitland do, however, need comment, viz., the association of Zr with muscovite+biotite at Whitland (Figs. 1, 2a), and

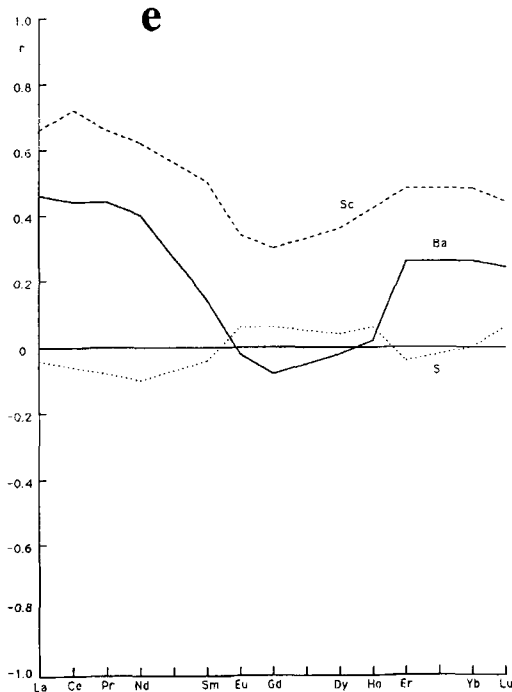


FIG. 2a-e. Correlation coefficients of rare earth elements with element/oxide concentrations and *d*-spacing intensities. 4.97–5.04 Å *d*-spacing represents muscovite+biotite, 6.39 Å albite, and 14.4 Å chlorite (see text).

the positive Ce anomaly in chlorite (Fig. 2b). In contrast to Cr and Ti, Zr is not a normal substitution in muscovite or biotite lattices (Deer *et al.*, 1992, p. 289). Its unexpected association with muscovite+biotite at Whitland is best explained by the inclusion of earlier formed crystals of zircon in (presumably detrital) biotite (Deer *et al.*, 1992, p. 25). Such inclusions would also explain the muscovite+biotite HREE enrichment at Whitland, zircon having a strong affinity for HREE (McLennan, 1989, fig. 9). The existence of zircon at Whitland is supported by calculations of the partial correlations of Zr with the REE after partialling out all the other elements of the correlation matrix: the resulting pattern (Zr* in Fig. 3) is very similar to published traces for zircon (e.g. McLennan, loc. cit.).

Positive Ce anomalies, as in the chlorite group at Whitland, are found today in ferromanganese nodules and crusts (Fleet, 1984, fig. 10.12; McLennan, 1989, p. 173) and in slowly accumulating oceanic sediments rich in authigenic metals (Thomson *et al.*, 1984, fig. 8). Although Fe, Mn and Cu are not especially enriched at Whitland (Temple and Cave, 1992, table 1), the positive Ce anomaly suggests that the Whitland chlorites may

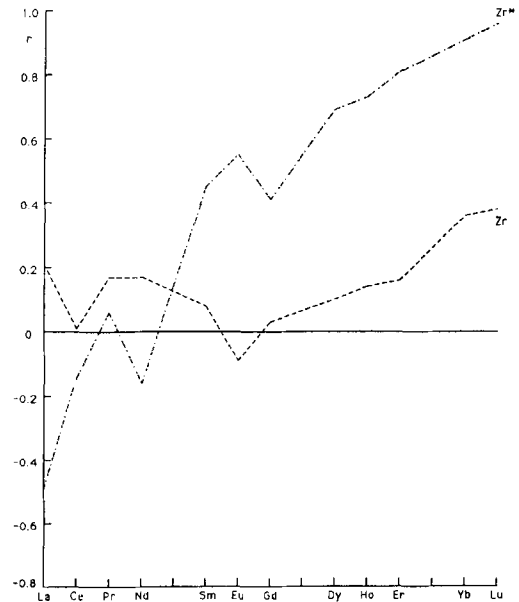


FIG. 3. Partial correlation coefficients of rare earth elements with Zr. The line Zr is from the 34-variate partial correlation matrix after partialling out *d*-spacings of 4.97–5.04 Å, 6.39 Å, 14.4 Å, P₂O₅ and CaO; the line Zr* is from the 13-variate correlation matrix after partialling out all other elements.

incorporate elements that originated as ferromanganese oxides.

The upwardly convex *REE* curves of the Whitland phosphate group (Fig. 2c) are broadly similar to the *REE* patterns described for the cores (but not the rims) of monazite nodules of probable diagenetic origin from the Lower Palaeozoic of Wales and elsewhere (Read *et al.*, 1987, fig. 2; Milodowski and Zalasiewicz, 1991, fig. 24). This similarity, together with the fact that Y belongs to the Whitland phosphate group, raises the possibility that incipient monazite-xenotime nodules might be present at Whitland. In detail, however, the patterns of Fig. 2c differ from described nodule patterns in having a negative Ce anomaly but lacking a Eu anomaly, and in these respects (and probably also in the absolute abundances they represent) they are closer to the curves for diagenetically altered biogenic apatites of widely different geological ages (Wright *et al.*, 1984, fig. 2; Elderfield and Pagett, 1986, figs. 5–6; Schmitz *et al.*, 1988, fig. 3; Grandjean and Albarède, 1989, p. 3182, figs. 1–2). The Whitland phosphate group is considered therefore to represent biogenic apatite. The upwardly convex *REE* curves of biogenic apatites have been attributed to uptake from sea water or from sedimented biogenic debris. Similar patterns — but without negative Ce anomalies — are however shown by partition coefficients of *REE* in some igneous apatites (Watson and Green, 1981, fig. 1). In all these apatites the *REE* are replacing Ca^{2+} , and yet the maximum *REE* enrichment occurs for *MREE* with ionic radii smaller than that of Ca^{2+} , rather than for *HREE* such as Ce^{3+} , Pr^{3+} or Nd^{3+} which are closer in size to Ca^{2+} . The same is true of diopside, where *REE* replacement of Ca^{2+} at the *M2* site is at a maximum for Gd^{3+} (Reitan *et al.*, 1980, fig. 1); and a similar phenomenon is shown by *REE* partition coefficients in hornblende (Jensen, 1973, figs. 5,11). It is not certain whether the size discrepancies in these cases are due entirely to the smaller cations fitting more optimally into the sites than the major cations that normally occupy them (Jensen, 1973, p. 2240; Reitan *et al.*, 1980, p. 189), or whether electrostatic or crystal field effects contribute to the phenomenon. The situation in apatite is complicated by the existence of two different Ca sites in the lattice, although the bond-valence calculations of Hughes *et al.* (1991, p. 1171, table 8) suggest that Nd should be the preferred *REE* occupant in both of them. It is difficult, therefore, to explain why biogenic apatites should sometimes be enriched in even heavier and smaller *REE* (maximum for Gd at Whitland and in Grandjean and Albarède, 1989, fig. 2).

The implications of the negative Ce anomaly in Whitland phosphates are debatable: although such an anomaly has been considered to imply an oxic environment (Elderfield and Pagett, 1986, fig. 13; Wright *et al.*, 1987, p. 639), other aspects of Whitland geochemistry suggest an anoxic environment (Temple and Cave, 1992, p. 591).

Acknowledgements

The Whitland specimens were collected by R. Cave and J.T.T. as part of their continuing study of the geochemistry and mineralogy of the Middle Ordovician Nod Glas sediments in Wales: field work was supported by a grant from the Central Research Funds of London University. C/S determinations were carried out by J.M. McArthur and A.T. Osborn, XRD analyses by S. Hirons, and specimen preparation by A. Carter. We have benefitted from discussions with H. Downes, M. Vickers and R. E. White. B. Roberts has continued to advise at all stages of the work. The support of NERC towards the ICPAES facilities at RHB New College (University of London) is gratefully acknowledged.

References

- Bish, D. L. and Chipera, S. J. (1988) Problems and solutions in quantitative analysis of complex mixtures by X-ray powder diffraction. *Advances in X-ray analysis*, **31**, 295–308.
- Cullers, R. L., Chaudhuri, S., Arnold, B., Lee, M. and Wolf, C. W. (1975) Rare earth distributions in clay minerals and in the clay-sized fraction of the Lower Permian Havensville and Eskridge shales of Kansas and Oklahoma. *Geochim. Cosmochim. Acta*, **39**, 1691–703.
- Deer, W.A., Howie, R.A. and Zussman, J. (1992) *The rock-forming minerals*, 2nd ed. Longmans, London, xvi + 696pp.
- Elderfield, H. and Pagett, R. (1986) Rare earth elements in ichthyoliths: variations with redox conditions and depositional environment. *The Science of the Total Environment*, **49**, 175–97.
- Elderfield, H. and Sholkovitz, E. R. (1987) Rare earth elements in the pore waters of reducing nearshore sediments. *Earth Planet. Sci. Lett.*, **82**, 280–8.
- Erel, Y. and Stolper, E. M. (1993) Modeling of rare-earth element partitioning between particles and solution in aquatic environments. *Geochim. Cosmochim. Acta*, **57**, 513–8.
- Fleet, A. J. (1984) Aqueous and sedimentary geochemistry of the rare earth elements. In *Rare earth element geochemistry* (P. Henderson, ed.), 343–73. Elsevier, Amsterdam.

- Grandjean, P. and Albarède, F. (1989) Ion probe measurement of rare earth elements in biogenic phosphates. *Geochim. Cosmochim. Acta*, **53**, 3179–83.
- Gromet, L. P., Dymek, R. F., Haskin, L. A. and Korotev, R. L. (1984) The North American Shale Composite: Compilation, major and trace element characteristics. *Geochim. Cosmochim. Acta*, **48**, 2469–82.
- Hughes, J. M., Cameron, M. and Mariano, A. N. (1991) Rare-earth-element ordering and structural variations in natural rare-earth-bearing apatites. *Amer. Mineral.*, **76**, 1165–73.
- Jensen, B. B. (1973). Patterns of trace element partitioning. *Geochim. Cosmochim. Acta*, **87**, 2227–42.
- McLennan, S. M. (1989) Rare earth elements in sedimentary rocks: influence of provenance and sedimentary processes. *Reviews in Mineralogy*, **21**, 169–200.
- MacRae, N. D., Nesbitt, H. W. and Kronberg, B. I. (1992) Development of a positive Eu anomaly during diagenesis. *Earth Planet. Sci. Lett.*, **109**, 585–91.
- Milodowski, A. E. and Zalasiewicz, J. A. (1991) Redistribution of rare earth elements during diagenesis of turbidite/hemipelagite mudrock sequences of Llandoverly age from central Wales. In *Developments in Sedimentary Provenance Studies* (Morton, A. C., Todd, S. P. and Haughton, P. D. W., eds.). Geological Society Special Publication, **57**, 101–24.
- Murray, R. W., Buchholtz ten Brink, M. R., Brumsack, H. J., Gerlach, D. C. and Russ, G. P. III (1991) Rare earth elements in Japan Sea sediments and diagenetic behavior of Ce/Ce*: results from ODP Leg 127. *Geochim. Cosmochim. Acta*, **55**, 2453–66.
- Read, D., Cooper, D. C. and McArthur, J. M. (1987) The composition and distribution of nodular monazite in the Lower Palaeozoic rocks of Great Britain. *Mineral. Mag.*, **51**, 271–80.
- Reitan, P. H., Roelandts, I. and Brunfelt, A. O. (1980) Optimum ionic size for substitution in the M(2)-site in metamorphic diopside. *Neues Jahrb. Mineral., Mh.*, 181–91.
- Roaldset, E. (1975) Rare earth element distributions in some Precambrian rocks and their phyllosilicates, Numedal, Norway. *Geochim. Cosmochim. Acta*, **39**, 455–69.
- Roberts, B., Morrison, C. and Hiron, S. (1990) Low grade metamorphism of the Manx Group, Isle of Man: a comparative study of white mica 'crystallinity' techniques. *J. Geol. Soc., London*, **147**, 271–7.
- Schmitz, B., Andersson, P. and Dahl, J. (1988) Iridium, sulfur isotopes and rare earth elements in the Cretaceous-Tertiary boundary clay at Stevens Klint, Denmark. *Geochim. Cosmochim. Acta*, **52**, 229–36.
- Taylor, J. C. and Zhu Rui (1992) Simultaneous use of observed and calculated standard profiles in quantitative XRD analysis of minerals by the multiphase Rietveld method: the determination of pseudorutile in mineral sands products. *Powder Diffraction*, **7**, 152–61.
- Taylor, S. R. and McLennan, S. M. (1985) *The continental crust: its composition and evolution: An examination of the geochemical record preserved in sedimentary rocks*. Blackwell Scientific Publications, Oxford, xv + 312 pp.
- Temple, J. T. and Cave, R. (1992) Preliminary report on the geochemistry and mineralogy of the Nod Glas and related sediments (Ordovician) of Wales. *Geol. Mag.*, **129**, 589–94.
- Thompson, M. and Walsh, J. N. (1988) *The Handbook of Inductively Coupled Plasma Spectrometry*, 2nd ed. Blackie, Glasgow, vi + 316 pp.
- Thomson, J., Carpenter, M. S. N., Colley, S., Wilson, T. R. S., Elderfield, H. and Kennedy, H. (1984) Metal accumulation rates in northwest Atlantic pelagic sediments. *Geochim. Cosmochim. Acta*, **48**, 1935–48.
- Walsh, J. N., Buckley, F. and Barker, J. (1981) The simultaneous determination of the rare-earth elements in rocks using inductively coupled plasma source spectrometry. *Chem. Geol.*, **33**, 141–53.
- Ward, C. D., McArthur, J. M. and Walsh, J. N. (1992) Rare earth element behaviour during evolution and alteration of the Dartmoor Granite, SW England. *J. Petrol.*, **33**, 785–815.
- Watson, E. B. and Green, T. H. (1981) Apatite/liquid partition coefficients for the rare earth elements and strontium. *Earth Planet. Sci. Lett.*, **56**, 405–21.
- Wright, J., Seymour, R. S. and Shaw, H. F. (1984) REE and Nd isotopes in conodont apatite: variations with geological age and depositional environment. *Geol. Soc. Amer. Spec. Paper*, **196**, 325–40.
- Wright, J., Schrader, H. and Holser, W. T. (1987) Paleoredox variations in ancient oceans recorded by rare earth elements in fossil apatite. *Geochim. Cosmochim. Acta*, **51**, 631–44.

[Manuscript received 9 March 1993:
revised 19 February 1994]